Proceedings of the Institute of Acoustics

A REVIEW OF SURFACE DUCT DECAY CONSTANTS

M N Packman
YARD Ltd, 233 High Holborn, London, WC1V 7DJ

1. INTRODUCTION

The existence of underwater sound channels has long been known, and their ability to trap sound and so enhance long range propagation has been well studied (Ref 1, pp147, and references therein). It is equally well known that sound is not perfectly confined in these waveguides and that a certain amount of acoustic energy leaks out of the duct, rendering them ineffective at low frequencies. This leads to the concept of a cut-off frequency, below which ducted propagation does not occur.

The amount of duct leakage is, as shown below, controlled by the imaginary part of the horizontal wavenumber, the so-called decay constant. This is a difficult quantity to calculate. An exact expression would require a complete analytical solution of the Helmholtz eigenvalue problem, but unfortunately this has not proved possible. Numerical solutions to this problem have been found for certain bilinear ducts (Ref 2, 3), but these are of limited application; approximate analytic formulae have been obtained via the WKB method (Refs 4, 5), but these are restricted to a limited range of frequencies; and a variety of empirical formulae exist (Ref 6, 7), fitted from physical or computer-generated data, but these too cannot be universally applied to any duct.

In this paper, we present a new expression for the surface duct decay constant, based on the WKB approximation (eg Ref 8, Ch 6.7) but extended to cover all frequencies. It is valid for realistic bilinear surface ducts, ie, the gradients in and below the duct are of the same order of magnitude, and it predicts leakage at all frequencies, both above and below a cut-off frequency which arises from the derivation of the constant. As such, it is an improvement on existing formulae, as we shall demonstrate. This constant is used in the propagation loss model INSIGHT (Ref 9).

2. INSIGHT DECAY CONSTANT

2.1 Formulation

The INSIGHT decay constant at frequency f for a duct of depth H, surface sound speed c_0, and sound speed gradients in and below the duct of magnitude c_1', c_2', is given in units of inverse length by

$$\alpha_1 = \frac{1}{4}\left(\frac{c_1'}{2c_0H}\right)^{\frac{1}{2}} e^{-\beta(f)} \qquad (1)$$

where

$$\beta(f) = \begin{cases} 3\pi\zeta(f) & f \geq f_1 \qquad (2a) \\ 3\pi\left[\zeta'(f_1)(f - f_1) + \zeta(f_1)\right] & f \leq f_1 \qquad (2b) \end{cases}$$

A REVIEW OF SURFACE DUCT DECAY CONSTANTS

and where

$$\zeta(f) = \left[(f/f_0)^{\frac{2}{3}} - 1\right]^{\frac{3}{2}}, \qquad f \geq f_0 \tag{3a}$$

$$\zeta'(f) = \frac{d}{df}\zeta(f). \tag{3b}$$

Also, f_0, which will be interpreted as the cut-off frequency, and f_1 are given by

$$f_0 = \frac{9}{8}c_1'\left(\frac{c_0}{2c_1'H}\right)^{\frac{3}{2}}, \tag{4}$$

$$f_1 = f_0\left(1 + \frac{3}{2}(9\pi)^{-\frac{2}{3}}\right) \doteq 1.16\, f_0. \tag{5}$$

(Throughout this paper, decay constants are denoted by α, with a subscript to indicate the author or model.)

2.2 Derivation

The well-known normal mode solution for the acoustic pressure field is (Ref 9, p122), using the asymptotic form of the Hankel function, and with a complex horizontal wavenumber $\kappa_n = \xi_n + i\alpha_n$,

$$p = (2\pi i)^{\frac{1}{2}} \sum_n \phi_n(z_s)\,\phi_n(z_r)\,e^{-\alpha_n r}\,\frac{e^{i\xi_n r}}{(\kappa_n r)^{1/2}}$$

Each mode of the field decays exponentially at a rate given by α_n. Hence we identify the decay constant of the n'th mode with the imaginary part of its horizontal wavenumber. In what follows we shall assume that $|\alpha_n| << |\xi_n|$ and so $|\kappa_n|^2 \sim \xi_n^2$. Also, for the small grazing angles of rays in a surface duct, $k^2 \sim |\kappa_n|^2$.

Substituting the approximate identity

$$\alpha_n = \mathrm{Im}(\kappa_n) \doteq \frac{\mathrm{Im}(\kappa_n^2)}{2\,|\kappa_n|}$$

into the WKB approximation (Ref 2, Sec 2.8, Eq 278)

$$\left|\frac{\mathrm{Im}(\kappa_n^2)}{\kappa_n^2}\right| \doteq \frac{e^{-2\int_{z_{1n}}^{z_{2n}} |\gamma_n(z)|\,dz}}{k\Gamma_n}$$

we obtain

A REVIEW OF SURFACE DUCT DECAY CONSTANTS

$$\alpha_n = \frac{e^{-2\int_{z_{1n}}^{z_{2n}} |\gamma_n(z)|\,dz}}{2\Gamma_n}, \tag{6}$$

where γ_n is the vertical wavenumber, Γ_n the cycle distance, and z_{1n}, z_{2n} the modal turning points.

Now, as frequency is increased from zero in a surface duct, the channel will start to support a mode structure. The first mode to be trapped as frequency increases is the lowest order (n=1) mode of Eq 6; at higher frequencies, higher order modes also become trapped, and the duct is referred to as cut-on. From the point of view of duct leakage, the critical frequency is that at which just one mode is trapped and dominates the sound intensity. Accordingly, we shall concentrate on this first mode only, and its attenuation constant α_1 will be referred to as the decay constant of the duct.

Specialising to the bilinear duct with wavenumber profile

$$k^2(z) = \begin{cases} k_0^2\left(1 - \frac{2c_1'}{c_0}z\right) & 0 \le z \le H \\ k_H^2\left(1 + \frac{2c_2'}{c_0}(z - H)\right) & z \ge H \end{cases} \tag{7}$$

the exponent of Eq (6) becomes, to first order in c_1', c_2' (dropping the n=1 subscript)

$$-2\int_{z_1}^{z_2} |\gamma(z)|\,dz = \frac{1}{3}\frac{c_0}{k_0^2}\left(\frac{1}{c_1'} + \frac{1}{c_2'}\right)\left[(\kappa^2 - k_0^2) + (k_0^2 - k_H^2)\right]^{\frac{3}{2}} \tag{8}$$

The first eigenvalue is given by the WKB approximation (Ref 9 Eq (6.7.10), p132) as

$$k_0^2 - \kappa^2 = \left(\frac{9\pi}{4}\frac{c_1' k_0^2}{c_0}\right)^{\frac{2}{3}} \tag{9}$$

Using Eq (9) in Eq (8) gives

$$-2\int_{z_1}^{z_2} |\gamma(z)|\,dz = \frac{3\pi}{2}(1 + c_1'/c_2')\left[(f/f_0)^{\frac{2}{3}} - 1\right]^{\frac{3}{2}} \qquad f \ge f_0. \tag{10}$$

As we shall discuss in Sec 3.2, f_0 is the dominant parameter in this expression, and gradient dependence should be contained within it. Thus, we can approximate $(1 + c_1'/c_2')$ by 2, ie. put $c_2' = c_1'$, which is approximately true for realistic ducts, with little error to α_1.

The cycle distance for a ray of surface grazing angle θ is

$$\Gamma = \frac{2c_0}{c_1'}\tan\theta \doteq \frac{2c_0}{c_1'}\sqrt{\frac{2c_1' z_1}{c_0}} \tag{11}$$

For rays trapped in the duct, the turning point z_1, at which $\gamma(z_1)=0$, satisfies $z_1 \leq H$. We shall use $z_1=H$ in this expression at all frequencies. This gives improved behaviour at low frequencies, i.e. a non-zero constant at $f = 0$, and induces little error since the exponent is the dominant factor. Substituting Eqs (10), (11) into Eq (6) gives the expression

$$\alpha = \frac{1}{4}\sqrt{\frac{c_1'}{2c_0H}}\,e^{-3\pi\zeta(f)}. \qquad (12)$$

This WKB expression Eq (12) is shown in Figure 1. It has two obvious defects; it holds for inflection at $f=f_0$. Both these defects arise because of the nature of the function $\zeta(f)$, and we seek to modify ζ as a cure.

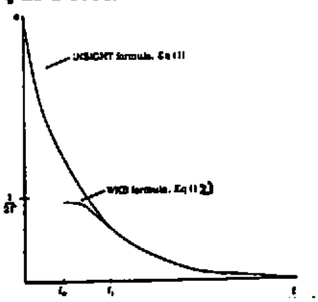

Figure 1

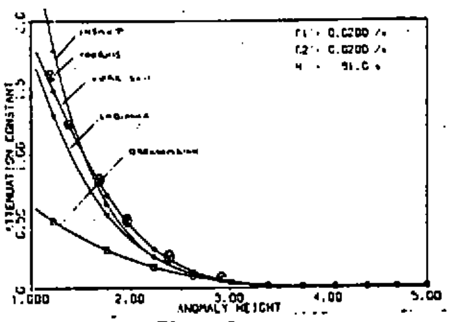

Figure 2

We accept Eq (12) for the region $f>f_1$ where the gradient of α is increasing; at $f=f_1$, the gradient of α is a minimum. Attempting to reproduce the Kerr curves of Sec 3.1, we wish to avoid the decreasing gradient for $f<f_1$, and so we choose to adopt a linear continuation of $\zeta(f)$ for frequencies $f<f_1$, continuous in both value and gradient at $f=f_1$. That is, if we define the function $\beta(f)$ as in Eq(2), then we redefine the decay constant to be

$$\alpha_l = \frac{1}{4}\sqrt{\frac{c_1'}{2c_0H}}\,e^{-\beta(f)}. \qquad (13)$$

Elementary calculus shows that f_1 must solve

$$9\pi\left[(f_1/f_0)^{\frac{2}{3}} - 1\right]^{\frac{3}{2}}(f_1/f_0)^{\frac{2}{3}} - 1 = 0,$$

and Eq(5) gives the approximate unique solution of this.

This continued expression Eq (13) is also plotted in Figure 1. We can see that we have solved both problems: α_l has a monotonic gradient (as does β), and is defined for all frequencies.

We interpret f_0 as the cut-off frequency of the duct. This is because the function $\zeta(f)$ appearing in the definition of α_l (Eq 3a) is defined only for $f \geq f_0$. At this frequency, $\zeta=0$, and the WKB expression, Eq (13), gives a decay constant of $1/(2\Gamma)$ or a pressure decrease of $1/e$ every ray cycle.

One can also show that f_0 is the frequency at which the WKB eigenvalue is equal to the wavenumber minimum, $\kappa^2=k_H^2$; or equivalently, at which the modal turning point is at the duct bottom, ie, $z_1=H$.

3. COMPARISON WITH OTHER DECAY CONSTANTS

Having presented the INSIGHT decay constant, it is time to discuss its accuracy. A variety of alternative expressions for the decay constant exist, and we present a survey of some of these here. This is by no means exhaustive, but it provides a framework in which to judge the validity of α_I. Classifying these alternative expressions as numerical, analytic and semi-empirical, we proceed to a step-by-step justification of α_I.

3.1 Exact Numerical Solutions

Kerr (Ref 2, p161, Fig 2-30) displays curves of attenuation constant $C=2\alpha(q_1{}^2k_0)^{-1/3}$ against anomaly height $g=H(q_1k_0{}^2)^{1/3}$, $(q_1=2c_1'/c_0)$ for a discrete set of values of $s=-(c_1'/c_2')^{1/3}$. These curves are obtained by numerical solution of the exact eigenvalue problem, and have the property that they give the decay constant α_K for **any** duct with the given s, ie, variable c_1', c_2', H such that $c_1'/c_2'=-s^3$. There is some scale invariance in the problem, which is characterised by the dimensionless parameters C and g. These quantities have the useful property that the cut-off frequency f_0 corresponds to the constant value $g=(9\pi/8)^{2/3} = 2.32$.

We consider these curves as giving the correct decay constant, and being the result with which to compare all other decay constants. However, they do have drawbacks: they are not curves of analytic expressions and they are limited to the values of s given in Ref 2. Surface ducts must have $s<0$, and realistic surface ducts have $c_2' > c_1'$, ie $-1 < s < 0$, but Kerr gives no curves for this range of s. Interpolation in s is ruled out as we do not know the s dependence. There is no reason to suppose a linear dependence; it is likely to be more complicated than this. Thus we are forced to find alternative representations of the decay constant.

Another numerical solution for the constant is given by Voorhis (Ref 3), again in the form of a set of curves, for various realistic discrete values of H, c_1' and c_2'. These do not explicitly exhibit the dimensionless behaviour of the Kerr graphs, but plot instead α_V (in dB/kyd) against frequency for different duct parameters. The Voorhis $s=-1$ curves agree perfectly with α_K at $s=-1$ (see Figure 2). Thus, these curves also provide essential checks on any analytic expression, but suffer from the same drawback as the Kerr curves when being considered as predictive tools.

3.2 Analytic Solutions

Analytic approximations to the numerical solutions are obviously desirable. We present three such, and compare them with the exact solutions.

3.2.1 INSIGHT

This is given by Eq (1) above.

3.2.2 Labianca

Labianca gives a decay constant (Ref 4, Eq 31c) which, in our notation, reads

$$\alpha = \frac{1}{2c_0}\left(\frac{c_1'^2}{9}\right)^{\frac{1}{3}} f^{\frac{1}{3}} e^{-\frac{3\pi}{2}\left(1+\frac{c_1'}{c_2'}\right)\zeta(f)} \qquad f \geq f_0$$

We extend this to the whole frequency range in the same manner as for α_I, ie, replace the function $\zeta(f)$ by $\beta(f)$, giving

$$\alpha_L = \frac{1}{2c_0}\left(\frac{c_1'^2}{9}\right)^{\frac{1}{3}} f^{\frac{1}{3}} e^{-\frac{1}{2}\left(1+\frac{c_1'}{c_2'}\right)\beta(f)} \tag{14}$$

3.2.3 Brekhovskikh

Brekhovskikh derives an energy reflection coefficient for the bottom of a surface duct (Ref 5, Eq 24.32, 24.42),

$$R^2 = \left(1 + e^{-2\int_{z_1}^{z_2} |\gamma(z)|\,dz}\right)^{-1}$$

in our notation. Equating this reflection coefficient to a corresponding decay term in the intensity, ie, $R^{2n} = e^{-2\alpha r}$ where n is the number of reflections, $n=r/\Gamma$, we obtain

$$\alpha = \frac{1}{2\Gamma}\ln\left(1 + e^{-2\int_{z_1}^{z_2} |\gamma(z)|\,dz}\right).$$

This can be evaluated in the same way as Eq (6) and extended to all frequencies giving

$$\alpha_B = \frac{1}{2\Gamma}\ln\left(1 + e^{-\frac{1}{2}\left(1+\frac{c_1'}{c_2'}\right)\beta(f)}\right) \tag{15}$$

We now have three analytical expressions for the decay constant - α_I, α_L, α_B - to compare with the numerical solutions α_K, α_V.

Figure 2 displays all five constants for a duct with $H = 91$m, $c_1' = c_2' = 0.02s^{-1}$, ie $s=-1$. (Of course, α_K depends only on s, not the precise values of H, c_1', c_2', but this is not so for the other constants.) The numerical curves α_K, α_V are in good agreement, as we would expect for exact solutions. Of the analytical curves, α_I and α_L agree well with the Kerr curve; α_B diverges for low values of anomaly height, though agreement is good above the cut-off frequency, at $g=(9\pi/8)^{2/3}$. At $s=-1$, then, both INSIGHT and Labianca constants seem accurate.

Physical values of s are used for the Voorhis curves, and the analytical formulae can be compared against these. Figure 3 shows curves for a duct with H=91m, $c_1'=0.02s^{-1}$, $c_2'=0.05s^{-1}$, ie $s=-0.74$. This time the numerical curve appears shifted to the right, and the analytical curves are little changed from their s=-1 values. Agreement is still good. Comparisons with Voorhis curves at other values of H, c_1' and c_2' show similar agreement, provided s is not too small or too large in magnitude. The universal nature of the Kerr curves ensures that we can extrapolate this agreement to all duct depths and gradients for this range of the parameter s. When $s<-1$ or $\simeq 0$, α_I is less accurate, but by (empirically) redefining f_0, agreement can be recovered. This is a question for further theoretical investigation.

Of the three analytical formulae, then, we can dismiss the Brekhovskikh constant as being a less accurate formula. There is little to choose between the INSIGHT and Labianca expressions regarding agreement with the numerical results. We prefer the INSIGHT decay constant, because $\alpha_L \to 0$ erroneously as $f \to 0$.

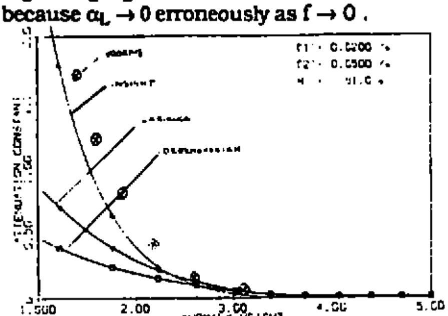

Figure 3

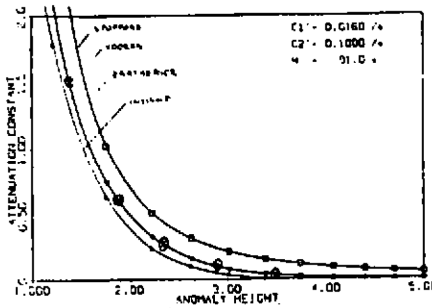

Figure 4

3.3 Empirical Solutions

Two semi-empirical decay constants are presented, one due to Bartberger (Ref 6, App J) and derived from transmission loss data generated by the normal mode computer model of NAVAIRDEVCEN; the other to Spofford (Ref 7), and used by the program FACT. They are, respectively, in decibels per yard,

$$\alpha_{Ba} = \frac{1}{1000} e^{a+b} \mathrm{dB/yd} \tag{16}$$

where

$$a = 3.7(H/100)^{-0.1586} \tag{17a}$$

$$b = 3.27n + 0.7965e^{2.78n - 10.422n^2} \tag{17b}$$

with

$$n = \frac{1}{4} + \frac{4}{3}\left(\frac{2c_1' H^3}{c_0^3}\right)^{\frac{1}{2}} f; \tag{18}$$

and, in decibels per nautical mile,

$$\alpha_S = \frac{14.88 \times 10^5}{20 \log_{10} e} \left(\frac{f}{1000}\right)^{-\frac{5}{3}} \frac{c_2'^{-\frac{1}{3}}}{H^3} \mathrm{dB/nm}. \tag{19}$$

Both expressions have units of H in feet; c_0 in ft s^{-1}; f in Hz; c_1', c_2' in s^{-1}. The Spofford constant is independent of c_1', and we assume that it is derived for an isothermal duct, ie c_1'=0.016s^{-1};

A REVIEW OF SURFACE DUCT DECAY CONSTANTS

Bartberger specifies that his constant is derived for a duct with $c_2'=0.15s^{-1}$. They are therefore somewhat limited in application.

Figure 3 shows α_{Ba} and α_S, along with α_I and α_V, for a duct of depth 91m, gradients $c_1'=0.016\ s^{-1}$, $c_2'=0.1s^{-1}$, which approximately satisfies the criteria for the empirical expressions. We can see that while the Spofford curve agrees well with Voorhis at low frequency, it is too high at high frequency. In dB units, this discrepancy can be excessive, especially in shallow ducts because of the H^{-3} dependence. Bartberger's expression is an excellent fit to the Voorhis curve at all frequencies for this duct. It is, however, constrained to the fixed gradient $c_2' = 0.1\ s^{-1}$. Also, the analytic expression for α_{Ba}, Eq (16), is highly unphysical - interpretation is difficult. For these reasons we favour α_I rather than the empirical constants.

4. CONCLUSION

To sum up our logic, the numerical solutions α_K and α_V are unsuitable as predictive decay constants because of their discreteness in the duct parameters. They do, however, serve as the baseline by which to judge other decay constants. Of the analytical formulae, α_B is inaccurate at low frequencies, α_L at very low frequencies, while α_I is correct through and above cut-off and plausible elsewhere. The empirical formulae α_S and α_{Ba} are discounted for having fixed gradients and/or for being in bad agreement with the baselines. The INSIGHT expression appears to be superior on all counts.

Further theoretical developments could lead to a decay constant for non-linear surface ducts, and for underwater channels. One could also investigate the theoretical reason for the necessary modifications of the cut-off frequency at small and large values of $|s|$ perhaps using exact Airy function eigenfunctions.

ACKNOWLEDGEMENT

This work has been carried out with the support of the Procurement Executive, Ministry of Defence.

REFERENCES

1) "Principles of Underwater Sound", R J Urick, 1975, McGraw-Hill.
2) "Propagation of Short Radio Waves", ed D E Kerr, 1951, McGraw-Hill.
3) "Experiment on Propagation in Surface Sound Channels", A C Kibblewhite and R N Denham, JASA **38**, 63-71 (1965).
4) "Normal Modes, Virtual Modes and Alternative Representations in the Theory of Surface-duct Sound Propagation", Frank M Labianca, JASA 53(4) 1973.
5) "Waves in Layered Media", L Brekhovskikh, 1980, Academic Press.
6) "The FACT Model", C W Spofford, May 1974, Maury Center Report 109.
7) "PLRAY - A Ray Propagation Loss Program", C Bartberger, Oct 1978, NADC - 77296 - 30.
8) "Fundamentals of Ocean Acoustics", L Brekhovskikh and Yu Lysanov, Springer-Verlag, 1982.
9) "INSIGHT: A Fast, Robust Propagation Loss Model Providing Clear Understanding", C H Harrison, UDT, 7-9 Feb 1990, London.

Proceedings of the Institute of Acoustics

IDENTIFICATION OF THE ACOUSTIC OCEAN TRANSFER FUNCTION IN THE TYRRHENIAN SEA

L Ju Fradkin

Ocean Acoustics Group, Department of Applied Mathematics and Theoretical Physics, University of Cambridge, Cambridge, UK

1. INTRODUCTION

The knowledge of the acoustic ocean transfer function (OTF) can be of interest in communications and when validating models of ocean environment. So far most authors, both those who employ ray-tracing and those who do acoustic signal processing have considered the problem in the approximation of geometrical optics. It is well known that in this approximation the received signal (otherwise known as response) can be modeled as the sum of attenuated and delayed copies of a transmitted signal (otherwise known as signature). We have shown in Fradkin[1] that formally the same is true in the presence of the first-order diffraction effects (the parabolic approximation). The only difference is that in this case each of the macropaths of the geometrical optics approximation is surrounded by a bundle of the so-called micropaths, and the sum over all macro- and micropaths can be viewed as an approximation to a corresponding (path) integral. Thus, mathematically speaking, the response is a convolution of the signature with an (ocean) transfer function.

It is also well known that in general, in the absence of further relevant information, the mathematical problem of deconvolution (in this case, identification of the ocean transfer function on the basis of signature/response measurements) is ill-posed [2, 3]. However, for some types of signal or noise, identification can be achieved. For example, OTF identification can be carried out when the signature possesses a bandwidth comparable to that of the OTF and nearly flat density spectrum as in Williams and Battestin[4]. This method does not rely on geometrical optics approximation and is easily generalized to non-flat density spectra. On the other hand, the restriction on bandwidth is crucial.

In this paper we discuss some statistical and some physical considerations behind a novel approach to the OTF identification in the framework of the first order diffraction theory. The statistical considerations are presented in full in Fradkin[5], and the physical ones in Fradkin[1]. The signals considered contain practically no low frequences and are broad-band, but we assume that their bandwidth is considerably smaller than the OTF's. We also assume that none of the paths deliver the signal with a reversed phase. The above assumptions appear to be reasonable *a priori* when, for example, only direct (deep sea) paths are considered. In this paper we report the results of applying the method to a representative signature/response pair collected during the Napoli 85 Trial (see Uscinski et al.[6]), with the response arriving along just such paths. The assumptions are validated *a posteriori* by showing that the resulting model is consistent with all the known facts.

2. DESCRIPTION OF THE PROBLEM AND A GENERAL APPROACH TO ITS SOLUTION

We have shown in Fradkin[1] that provided the ocean is non-dispersive, weakly irregular, and no phase reversal takes place during propagation,

IDENTIFICATION OF THE ACOUSTIC OCEAN TRANSFER FUNCTION

$$\tilde{r}_i = \sum_{n=N_o}^{N_1} K_n \, \tilde{s}_{i,n} \, \Delta\tau + \eta_i, \quad i = 0, \ \ldots, \ I - 1, \tag{1}$$

where I, N_o, and N_1 are natural numbers; the tilde, $\tilde{}$, indicates the measured signals contaminated with noise; $\tilde{r}_i \equiv \tilde{r}(t_{i+I})$ is the response measured at the moment $t_{i+I} = (i + I)\Delta\tau_o$; $\Delta\tau_o$ is the sampling interval; $\tilde{s}_{i,n} \equiv \tilde{s}(t_{i+I} - \tau_n) = \tilde{s}(t_{\beta(i+I) - n})$ is the signature measured or interpolated at the moment $t_{i+I} - \tau_n$; $\tau_n = n\Delta\tau$ is a delay in signal propagation; $\Delta\tau$ is the interpolation interval; β is the interpolation factor equal $\Delta\tau_o/\Delta\tau$; η_i is the composite error at the moment t_{i+I}; $K_n\Delta\tau$ is the unknown proportion of signature arriving with delays in $[\tau_n, \tau_n - \Delta\tau]$, so that

$$K_n \geq 0, \qquad \forall n = N_o, \ldots, \ N_1 \tag{2}$$

and with large probability, the L_1-norm for K,

$$||K||_1 \equiv \sum_{n=N_o}^{N_1} K_n \Delta\tau \leq \alpha, \tag{3}$$

where α is a number determined by the geometry of the problem and known *a priori* to data analysis. The signature, $\tilde{s}$, is assumed to be interpolated because often, and in particular in the case of the Napoli 85 Trial, the resolution required for the ocean transfer function, K, is finer than the sampling interval for $\tilde{s}$ and $\tilde{r}$.

The equation (1) describes $\tilde{r}$ as a (discrete) linear convolution of $\tilde{s}$ with K. The process of estimating K on the basis of (1) and known $\tilde{s}$ and $\tilde{r}$ is known as deconvolution. In general, deconvolution is an ill-posed problem, meaning that its solution, $\widehat{K}$, is sensitive to high-frequency errors in $\tilde{s}$ and $\tilde{r}$. It can be identified only if some powerful physical constraints are used.

When dealing with a particular deconvolution problem it is impossible to say *a priori* to data analysis what particular constraints may do the job. Several classes of constraints have been studied in the literature (e.g. Schafer et al.[3].) The general approach can be described as follows: to estimate K_n, $n \in [N_o, N_1]$ one has to minimize the cost function J_o described in (A.1) under some constraints. The solution should be accurate enough to produce reasonable residuals and to be reasonably close to its *a priori* estimate (if such is available). Also, it should be reasonably insensitive to various assumptions behind the mathematical model. The measures of what is "reasonable" should be available *a priori*, otherwise the problem cannot be solved. The requirements of accuracy and insensitivity are, as a rule, contradictory, and one can claim that the problem has been solved only if some trade-off can be achieved.

In this paper we describe a method for estimating K, that is $K_n, n \in [N_o, N_1]$ with N_o and N_1 also unknown. The only *a priori* restriction on N_o and N_1 is the following:

$$1 < N_o < N_1 < 2\beta I. \tag{4}$$

It is assumed that for negative i's the $\tilde{s}_i'$ are known (in our case we have taken them to be zero). The method is based on minimization of the cost function,

IDENTIFICATION OF THE ACOUSTIC OCEAN TRANSFER FUNCTION

$$J \equiv \sum_{i=0}^{I-1} \left(\tilde{r}_i - \sum_{n=N_o}^{N_1} K_n \, \tilde{s}_{i,n} \, \Delta\tau \right)^2 + \lambda^2 \sum_{n=N_o}^{N_1} K_n^2 \, \Delta\tau, \tag{5}$$

with respect to λ^2 and K under the Non-negativity constraint, (2), and the Bounded L_1-norm constraint, (3). The justification of the choice of the cost function (5) is given in Fradkin[5]. Two additional constraints are also employed. The first one is our estimate of the composite error variance:

$$\sum_{i=0}^{I-1} \left(\tilde{r}_i - \sum_{n=N_o}^{N_1} \hat{K}_n \, \tilde{s}_{i,n} \, \Delta\tau \right)^2 \approx \hat{\sigma}_\eta^2 . \tag{6}$$

The value of $\hat{\sigma}_\eta^2$ is based on independent data analysis and is discussed in Fradkin[5]. The second is the estimate of the maximum probable spread of the OTF corresponding to a single macropath,

$$\tau_{max}^1 = \tau_o . \tag{7}$$

The value of τ_o can be calculated by using physical considerations and ocean parameters as is done in Fradkin[1]. It is finite when the signals under consideration contain practically no low frequences. We call it the Maximum Probable Time Delay along a Direct Ray Tube and remark that it is akin to a Finite Support constraint (see Schafer et al.[3].) In addition to the above constraints, we have used analysis of residuals (goodness-of-fit) to assure that the estimated response reproduces the main features of the measured pulse, $\tilde{r}$.

The computational procedure is based on the algorithm offered in Butler et al. [2] and is described in Fradkin[5]. It is incorporated into the DECO package under the name of DECOP (for DECOnvolution for Positive transfer functions).

3. DESCRIPTION OF THE EXPLORATORY SIGNAL PROCESSING PROCEDURE

The Napoli 85 Trial was conducted in the central Tyrrhenian Sea in October 1985. Its full description can be found in Uscinski et al.[6]. The ocean parameters were such that at the distances of interest diffraction was small but not always negligible[9]. The schematic geometry of the Trial is presented in Fig. 1. The signal measured at point S close to the source is referred to everywhere below as the signature and the signal at point R is called response. A representative signature/response pair is shown in Fig. 2, and their discrete Fourier transforms, in Fig. 3. It is important to realize that all the signals were low-pass filtered and then digitized by the hardware, so that they contain I = 49 discrete points sampled at an interval of

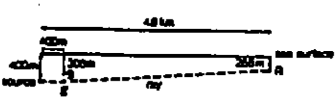

FIG. 1. Schematic geometry of the Napoli 85 Trial.

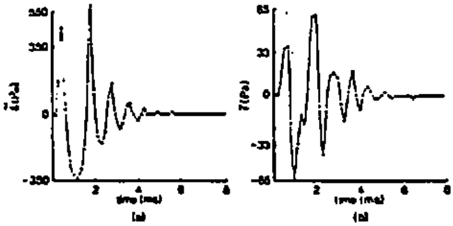

FIG. 2. A typical signature/response pair.

$\Delta\tau_o = 1/6$ ms. The low-pass filter had a cut-off frequency of 3 kHz and a very low accuracy between 2 and 3 kHz. We also have to emphasize that S does not lie on a ray connecting source to R, although it is reasonably close to it.

In order to identify the ocean transfer function from an $\tilde{s}/\tilde{r}$ pair we perform the following operations:

1. Pre-filter both $\tilde{s}$ and $\tilde{r}$ using a low-pass filter with the cut-off frequency of 2 kHz;
2. Interpolate both $\tilde{s}$ and $\tilde{r}$ using a spectral interpolator with the interpolation factor $\beta = 20$, making the time unit, $\Delta\tau = 1/120$ msec.
3. Set $N_o = 980$, $N_1 = 1099$, and $\lambda^2 = 0.01$.
4. Optimize J in (5) using the above values and DECOP.

The resulting ocean transfer function is presented in Fig. 4(b). It is non-negative and its L_1-norm,

$$\sum_{n=N_o}^{N_1} K_n \Delta\tau \approx 0.17. \tag{8}$$

The corresponding residual variance, $\hat{\sigma}_\eta^2$, is such that the relative error,

$$\hat{\sigma}_\eta/\sigma_{\tilde{r}} \approx 0.27, \tag{9}$$

where

$$\sigma_{\tilde{r}} \equiv [\frac{1}{I}\sum_{i=0}^{I-1}(\tilde{r}_i - \bar{r})^2]^{1/2}, \text{and} \bar{r} \equiv \frac{1}{I}\sum_{i=0}^{I-1}\tilde{r}_i.$$

The shape of the function suggests the existence of two macropaths leading from the source to R, with the maximum probable time delay along a direct macropath,

$$\tau^1_{max} \approx 4.10^{-5}\text{s}\ (\Delta n_1 = 5), \tag{10}$$

where Δn_1 is the width of the widest $\hat{K}$-peak in the interpolation time units ($\Delta\tau = 1/120$ msec). The need for pre-filtering and interpolation as well as the choice of the cost function J, all the constraints, λ^2, N_o and N_1 are all justified in detail in Fradkin[5] by exploratory data analysis. We only make the following points:

1. The pre-filtering is conducted, because the higher frequences in $\tilde{s}$ and $\tilde{r}$ as measured during the Napoli 85 Trial are heavily contaminated with noise, and $\hat{K}$-estimates are highly sensitive to high frequency errors.
2. The interpolation is conducted, since a much higher resolution is required for $\hat{K}$ than for $\tilde{s}$ and $\tilde{r}$.
3. The above-value of $N_o(= \beta I)$ is chosen on the assumption that the time of arrival of the response is larger than the signal's duration by at least $\Delta\tau$.
4. The above value of N_1 is chosen to be small enough to produce a smaller value of $||\hat{K}||_1$; larger values of N_1 lead only to the appearance of thin "tails" in the estimates of K (Fig. 4a), and by analyzing simulated data we found such tails to be symptomatic of N_1 being overestimated. On the other hand, if N_1 was reduced any further to cut off the second peak in the OTF estimate, the fitting qualities of the latter would suffer: in particular, the kink before the second peak in Fig. 2b would not be reproduced.
5. The above value of λ^2 is chosen so that the width of the first (widest) peak in Fig. 4(b) can equal the value τ_o in (10). With high probability, the latter can be considered to be the maximum probable time delay in propagation of acoustic waves along the path S′R as in Fig. 1 (see Fradkin[1]).

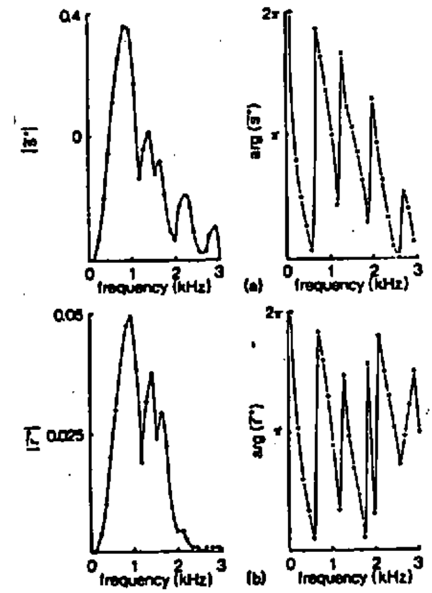

FIG. 3. Moduli and phases of the Fourier components of signature and response: (a) (i) moduli of the Fourier components of $\hat{s}$. (ii) phases of the Fourier components of $\hat{s}$; (b) (i) moduli of the Fourier components of $\hat{r}$. (ii) phases of the Fourier components of $\hat{r}$.

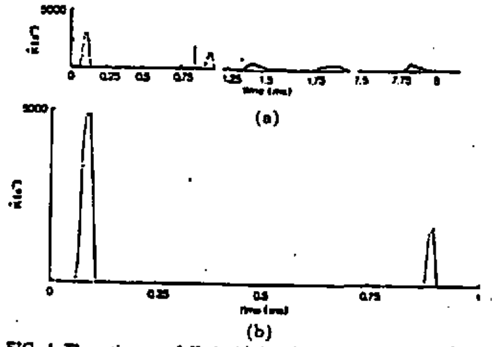

FIG. 4. The estimates of K obtained with DECOP and (a) $\lambda^2 = 0.01$, $N_0 = 980$, $N_1 = 1959$; (b) $\lambda^2 = 0.01$, $N_0 = 980$, $N_1 = 1099$.

Although the true width of the first peak can be somewhat different, our numerical experiments have shown that the general shape of $\hat{K}$ does not change with λ^2. The numerical experiments have also shown that λ^2 increases with τ_0 monotonically, so that the trial-and-error procedure required to find the correct value of λ^2 is not subjective.

6. The Non-negativity constraint is used because it allows the resulting estimate of the OTF to have a much higher frequency content (with the bandwidth of about 40 kHz) than that of signature and response. For comparison, the estimate obtained by assuming $\lambda^2 = 0$ and using DECON (for DE-CONvolution) - a routine in DECO minimising (5) without this or any other of the above constraints, is presented in Fig. 5. In this situation (5) achieves its minimum at

$$\widehat{K_i^*} = \tilde{r}_i^* / \tilde{s}_i^*, \tag{11}$$

where the star designates a Fourier component. It is interesting to note that the Fourier components of the OTF estimates obtained with and without the Non-negativity constraint coincide on the 300 - 1700 Hz interval (Fig. 6). The fact that they do not match at small frequences is not suprising, because both estimates fail there: the estimates obtained without the Non-negativity constraint, because at these frequences the Fourier components of $\tilde{s}$ are too small (see (11) and Fig. 3a), and the estimates obtained with the Non-negativity constraint because τ_0 is estimated assuming that the amount of energy at these frequences is negligible (see Fradkin[1]). The fact that they do not match at the higher frequences is not unexpected either, because the first estimate fails there for the same reason it fails at the smaller frequences (Fig. 3a). The reliability of the method incorporating the Non-negativity constraint has been tested by simulating a response, $\hat{r}$, on the basis of $\hat{s}$ in Fig. 2a and $\hat{K}$ in Fig. 4b, adding a random noise to both $\hat{r}$ and $\tilde{s}$, and applying DECOP to the resulting pair. The outcome of these simulations can be seen in Fig. 7.

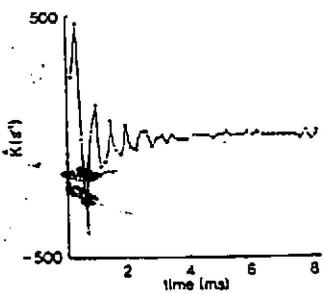

FIG. 5. The estimate of K obtained with DECON and $\lambda^2 = 0$.

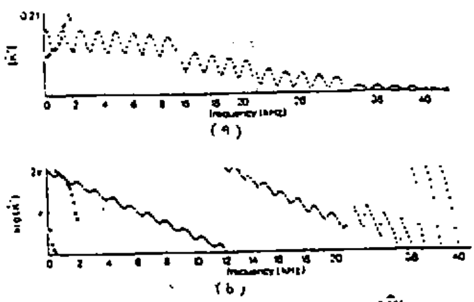

FIG. 6. Moduli and phases of the Fourier components of $\widehat{K}$ in Fig. 4(b) (·) and Fig. 5 (•), (a) moduli, (b) phases.

7. If there was only one macropath between S′ and R we would expect $||K||_1 \approx 0.1$, since $L'/L \approx 0.1$. But the OTF estimate depicted in Fig. 4(b) suggests the existence of two macropaths. Therefore, it is not surprising that a larger value appears in (13).
8. The relative error (14) seems a bit too large, but relative error is not a very good measure of fit when a large proportion of the signal is relatively small. The response predicted on the basis of $\tilde{s}$ in Fig. 2a and $\hat{K}$ in Fig. 4(b) actually fits the measured response rather well (Fig. 8). Also, it has been shown in Fradkin[5] that the relative error of this order is easily attributable to the low-pass filtering and/or positioning of the portable array employed in the Trial. The assumptionn that K is a function of the time difference only involves a model error too.

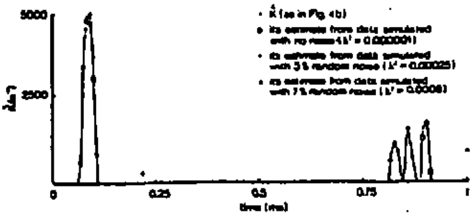

FIG. 7. Estimates of $\hat{K}$ in Fig. 4(b) obtained with simulated data, such that $\lambda_i = \Sigma \hat{K}_s \lambda_{i-s} \Delta\tau, i = 0,...,I-1$.

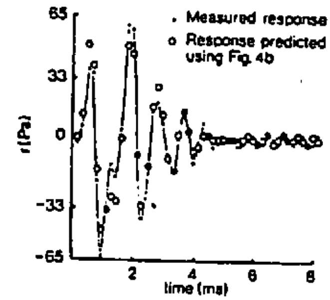

FIG. 8. Response predicted with $\hat{K}$ in Fig. 4(b) versus measured (and low pass filtered) response.

4. DISCUSSION

It is well known that the problem of optimizing the cost function (5) is ill-posed in the sense that the estimates are sensitive to errors in high frequencies. By conducting various numerical experiments with our data we have established that they allow for a reasonably reliable identification procedure based on low-pass filtering and utilization of the Non-negativity, Bounded L_1-norm and Maximum Delay along the Direct Raytube constraints. The necessity for low-pass filtering was dictated by the recording peculiarities of the Napoli 85 Trial and is not expected to arise every time the propagation of acoustic pulses is studied in the ocean. The Maximum Probable Time Delay along a Direct Raytube constraint is believed to be important only when working close to the geometrical optics limit, and it is applicable only when the signal does not contain low frequences. However, the Non-negativity and the Bounded L_1-norm constraints can have much wider applicability - in the situations where the signals possess a narrower frequency band than the ocean transfer function.

The main conclusion from the exploratory analysis of the Napoli 85 data is the presence of the second macropath. This can be validated independently on physical grounds by employing a model of the ocean fluctuations explaining them in terms of mixing intrusions [6, 1]. At first, we could not explain this result. To elaborate, given spectra of medium fluctuations and some mean parameters one can assess whether the existence of the second macropath is probable or not. Originally, it has been assumed that the medium fluctuations in the Tyrrhenian Sea were determined mainly by the internal waves. For the internal waves, a spherical source and $L \geq L_p$, the no-ray-intersection criterion reads as follows:

$$0.1 < \mu^2 > qL^2 L_p L_v^{-2} << 1, \tag{15}$$

where $< \mu^2 >$ is the variance of the irregular refractive index; q is the signal's wavenumber; L_p is the horizontal correlation strength (see Uscinski et al.[6]); and the numerical coefficient is due to the fact that the source is spherical. By analyzing the environmental data it has been found that for the Napoli 85 Trial, $< \mu^2 >= 0.5 \times 10^{-8}$; and by fitting the internal waves spectrum to these data the following estimates have been obtained:

$$L_v = 77 \text{ m}, \text{ and } L_p = 1052 \text{ m}$$

(B. J. Uscinski, pers. comm.) It is easy to check that for these values and frequences of about 1 kHz, criterion (15) is satisfied, and hence the appearance of the second macropath is highly improbable. However, the detailed analysis has shown that the internal waves model is inconsistent with the environmental data, and a new model involving mixing intrusions has been proposed in Uscinski et al.[6]. It is suggested that the intrusions lead to the presence of a long thin structure at a 270 to 330 m depth, with the speed of propagation lower than in the host medium by about 1 m/sec. This sort of a quasi-deterministic structure could well account for the existence of the secondary macropath mentioned above. Indeed, the preliminary calculations of the difference in the times of arrival of the first and second peak in Fig. 4(b) are of the correct order. This removes the original contradiction between the results of our signal processing procedure and the internal waves model of ocean fluctuations, and shows that in its turn, in the absence of good environmental data, such a procedure could be used for model verification purposes.

As to the accuracy of the ocean transfer function estimates, our experiments with simulated data suggest that the amplitude of the ocean transfer function in Fig. 4(b) is off by approximately 20%, and the accuracy of peak positions is $\pm\frac{1}{17}$ ms. The estimate of the OTF corresponding to the second macropath is expected to be corrupted more than the first one.

The method described in this paper is being now applied to process all the relevant pulses transmitted in the Trial, and the resulting conclusions will be reported shortly.

5. ACKNOWLEDGEMENTS

I would like to thank the Principal Investigators in the Napoli 85 Trial, Drs. T. E. Akal and B. J. Uscinski, for giving me permission to use the data, and Dr. J. Potter for providing me with the magnetic tapes and relevant information. I am also grateful to Dr. B. J. Uscinski and Professor T. E. Ewart for many helpful discussions on the physics of the ocean. This work has been supported by Marconi Maritime Applied Research (Cambridge) under Grant 08905.

6. REFERENCES

[1] L Ju Fradkin, 'Identification of the Acoustic Ocean Transfer Function in the Tyrrhenian Sea II: Physical Considerations', to appear in *J Acoust Soc Am* (1990)

[2] J P Butler, J A Reeds, and S V Dawson, 'Estimating Solutions of First Kind Integral Equations with Nonnegativity Constraints and Optimal Smoothing', *SIAM J Numer Anal* 18(3) pp381-397 (1981)

[3] R W Schafer, R M Mersereau and M A Richards, 'Constrained Iterative Restoration Algorithms', *Proc IEEE* 69(4) pp432-450 (1981)

[4] R E Williams, and H F Battestin, 'Coherent Recombination of Acoustic Multipath Signals Propagated in the Deep Ocean', *J Acoust Soc Am* 50, 6(1) pp1433-1442 (1971)

[5] L Ju Fradkin, 'Identification of the Acoustic Ocean Transfer Function in the Tyrrhenian Sea I: Statistical Considerations', to appear in *J Acoust Soc Am* (1990)

[6] B J Uscinski, J Potter, and T Akal 'Broadband acoustic transmission fluctuations in the Tyrrhemian Sea: Preliminary results and an arrival-time analysis', 86(2) pp706-715 (1989)